Chapter 4

Application of Metal-Semiconductor-Metal Photodetector in High-Speed Optical Communication Systems

Farzaneh Fadakar Masouleh and Narottam Das

Additional information is available at the end of the chapter

http://dx.doi.org/10.5772/58997

1. Introduction

Recently, there is a very strong interest towards the miniaturization of optical and electrical components with faster and more efficient performance which has incorporated new capabilities in various aspects including high-speed telecommunication systems [1]. Optical communication technology has greatly developed during recent years that affect all areas of the modern telecommunication systems. Photodetectors along with optical sources and fibers are regarded as integral part of all optical fiber communication systems [2]. The high bandwidth and/or the gain of photodetectors with the wavelength in the near-infrared region (0.8 to 1.6 μm) are quite important because of their ideal commercial and industrial usage in optical fiber communication systems. The photodetectors are known as optoelectronic devices that can convert the absorbed optical energy into electrical energy which usually appears as a photocurrent that can be used by telephone systems, computers, or other terminals at transmitting and receiving part of the communication systems [3]. There are many types of photodetectors depending on their application in optical communication systems, imaging systems, and so on. The sensitivity of detectors varies through different optical spectra, such as the infrared and ultraviolet. Semiconductor detectors are commonly used in optical fiber communication systems because they rely on internal photoelectric effect but there is no photoemission effect. They either work in photovoltaic mode as solar cells or in photoconductive mode as revers biased photodetectors [4]. Metal-semiconductor-metal photodetectors (MSM-PDs), positive-intrinsic-negative (pin) photodetectors, avalanche photodiodes and heterojunction PDs as solid state semiconductor devices are most widely used in high-speed optical communication systems. The MSM-PDs are attractive devices compared with other photodetector structures, for their remarkable high sensitivity-bandwidth product, ease of fabrication and ease of

integration with other components into monolithic receiver circuits. The MSM-PD consists of two identical Schottky contacts with interdigitated electrode configuration on top of an undoped semiconductor substrate, one of the contacts being forward and the other reverse biased. With fabrication of interdigitated electrodes the closely spaced fingers provide smaller transit time for the carriers as well as allowing a larger photo-absorption area for the device [5, 6]. The two Schottky barriers associated with the presence of contacts block current flow from the metal to the semiconductor which is the cause for the extremely low dark current observed in MSM-PDs. One important feature of the MSM photodetector is its low capacitance compared with a pin photodetector, (with an intrinsic region (i.e., undoped semiconductor) in between the n-and p-type semiconductors). The capacitance of a MSM photodetector with interdigitated electrodes is always smaller than that of a pin photodetector of equal light sensitive area and leads to very high-performance operation.

High speed photodetection manifests an exciting new paradigm for modern telecommunication systems. Advanced or modern optical systems, i.e., the ultrahigh-speed optical telecommunication systems, such as any typical fiber optic communication system consist of a transmitter, a data transmission media or channel (usually optical fiber, waveguide, and free space air-gap), and a receiver (pin photodiodes and photodetectors). The major part of the optical transmitter is a light source (laser or light-emitting diode (LED)), whose function is to convert an information signal from its electrical form into light. The photodetectors as an important part of receiver are used to convert an optical information signal back into an electrical signal. For higher speed and broader bandwidth applications in optical communications and interconnects, high-performance optical receivers are required and the MSM photodetector as the heart of optical receiver has many advantages such as wide bandwidth and low capacitance. MSM-PDs are promising candidates in optoelectronic integrated circuits. Also they have fast time response and very low dark current, as compared with other types of photodetectors.

The new field of plasmonics has received particular attention due to unique optical features of nano scale architectures in noble metals particularly silver and gold. The coherent oscillations of electrons as surface plasmons are strongly localized in the nanoscale at the metal-dielectric interface, and metal nanoparticles. When the losses are small enough, the surface plasmon resonances can occur. The metals with good quality for plasmonic applications should satisfy two properties such as $\varepsilon'_m < -1$, and $\varepsilon''_m << |\varepsilon'_m|$, where ε'_m, and ε''_m are real and imaginary parts of metal dielectric permittivity, respectively [7].

Dielectric and magnetic properties of the noble metals with nano-textured structure can easily be determined by implementation of Lorentz-Drude model [8]. Below plasma frequency, the good conductors like silver (Ag) and gold (Au) have negative values for the real part of complex dielectric constant. Therefore, it is necessary to define an appropriate model to specify the dielectric properties of the materials. A complex dielectric function for some metals and surface plasmas which have good agreement with the experimentally measured results can be expressed in the following form [9]:

http://dx.doi.org/10.5772/58997

$$\varepsilon_r(\omega) = \varepsilon_r^f(\omega) + \varepsilon_r^b(\omega) \tag{1}$$

where, the term $\varepsilon_r(\omega)$ is the complex dielectric function for metals, $\varepsilon_r^f(\omega)$ is referred to as free electron effects, and $\varepsilon_r^b(\omega)$ is associated with bound electron effects. This model takes both the intraband, $\varepsilon_r^f(\omega)$, and interband, $\varepsilon_r^b(\omega)$, effects into the account for simulations. The former, Drude model, can describe the transport properties of electrons in good conductors and the later, Lorentz model, is a semi-quantum model describing bound electron effects. The Drude and Lorentz model in frequency domain can be written in the following form of (2) and (3), respectively.

$$\varepsilon_r^f(\omega) = 1 + \frac{\Omega_p^2}{i\omega\Gamma_0 - \omega^2} \tag{2}$$

$$\varepsilon_r^b(\omega) = \sum_{m=1}^{M} \frac{G_m \omega_p^2}{\omega_m^2 - \omega^2 + i\omega\Gamma_m} \tag{3}$$

where, $\Omega_p = G_0^{1/2}\omega_p$ is the plasma frequency associated with intraband transitions with oscillator strength G_0 and damping constant Γ_0, while m is the number of oscillators with frequency ω_m and $1/\Gamma_m$ is the oscillator lifetime [10]. The following equation accounts for the complex index of refraction and dielectric constant of materials and can be represented as a combined form [11]:

$$\varepsilon_r(\omega) = \varepsilon_{r,\infty} + \sum_{m=0}^{M} \frac{G_m \Omega_m^2}{\omega_m^2 - \omega^2 + i\omega\Gamma_m} \tag{4}$$

where, $\varepsilon_{r,\infty}$ is the relative permittivity at infinite frequency, G_m is the strength of each resonance term, Ω_m is the plasma frequency, ω_m is the resonant frequency, and Γ_m is the damping factor or the collision frequency.

The frequency dependent Gold dielectric permittivity is complex and is obtained from Lorentz-Drude model, $\varepsilon_m = \varepsilon'_m + i\varepsilon''_m$. It consists of a large negative real part ε'_m and a small positive imaginary part ε''_m responsible for light absorption. The letter i is an imaginary unity. Gold dielectric constant varies for different frequency ranges.

For our simulation of plasmonic-base MSM-PD, the Lorentz-Drude model for gold is solved with 6 resonant frequencies (multi-pole dispersion). The simulation is performed over a constant plasma frequency which depends on the density of charge carriers with the amount of 0.137188E+17. The resonant frequency changes according to the resonance strength. The Lorentz-Drude material parameters are listed in the following Table-I.

Term	Strength	Resonant Frequency	Damping Frequency
0	0.7600	0.000000E+00	0.805202E+14
1	0.0240	0.630488E+15	0.366139E+15
2	0.0100	0.126098E+16	0.524141E+15
3	0.0710	0.451065E+16	0.132175E+16
4	0.6010	0.653885E+16	0.378901E+16
5	4.3840	0.202364E+17	0.336362E+16

Table 1. Lorentz-Drude parameters for gold (measured in radians per second).

Investigation on the optical properties of the nano-structures is crucial for the design of optical devices. Next generation information and communication technologies are under direct influence of nano-plasmonic devices because of their unique properties that hold promise for potential applications in various fields of technology, properties such as overcoming the diffraction limit, efficiency in confinement of light at subwavelength scale, and ultrahigh speed signal transport with the same order as the speed of light make them vigorous devices.

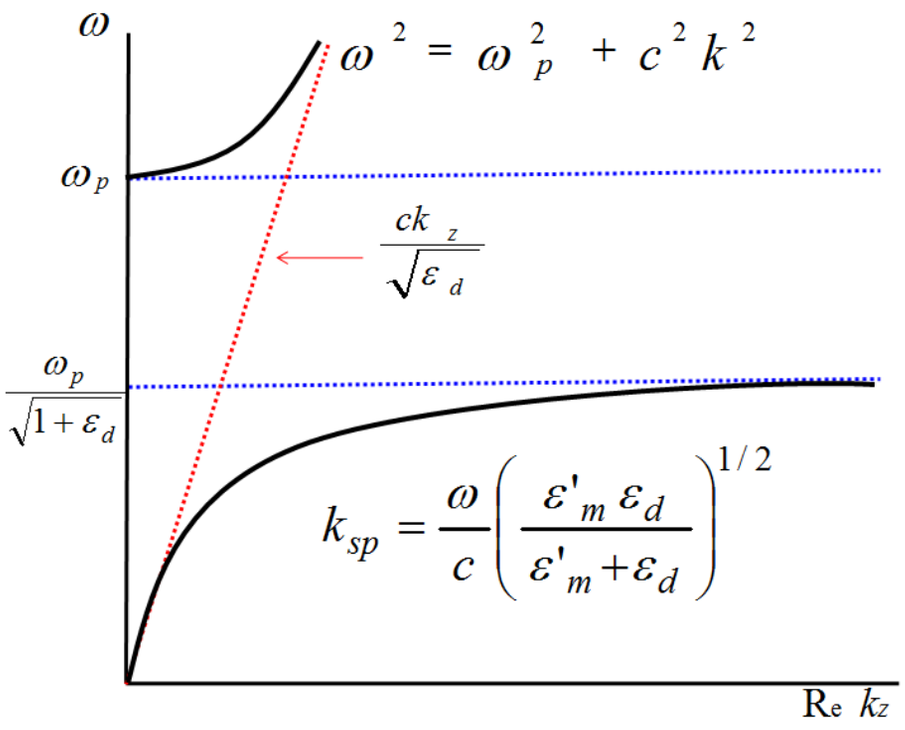

Figure 1. The dispersion relation of non-radiative SPs on the right of the light line and dispersion relation of radiative SPs on the left of the light line.

There has been a considerable and growing interest to clarify all phenomena corresponding to the improvement in light absorption via nano-scale structuring recently [12-15]. Over the

http://dx.doi.org/10.5772/58997

decade, an interesting effect of light interacting with metallic structures has been revealed. For sufficiently small nano-grating period, higher order diffractions are suppressed and only the zero order diffraction is present. The main motivation is to come up with a practical method to avoid the undesirable light reflection from the surface of the electrodes and enhance the light transmission efficiency through the subwavelength aperture.

It is useful to describe the SP dispersion relation as shown in Fig. 1. To have propagating bound SPs, the wave vector component must be real along the interface. Any light cannot be used for SP generation, because the real part of the wave vector in the z-direction exceeds that of free light ($\omega=ck$) as shown in Fig. 1 and a coupling mechanism is required. In the presence of a transverse magnetic (TM) polarized light, the SPs exist along a metal-dielectric interface. There are several techniques to excite the SP waves, such as prism coupling and grating coupling. For the case of semiconductors, prism coupling is not very much advantageous. The attention should be paid to prism refractive index which is hardly higher than popular semiconductors used for corresponding researches [16, 17].

2. Nano-gratings structures and operation principles

The metallic nano-gratings can exhibit absorption anomalies. One of these particularly remarkable anomalies is the surface plasmon polariton (SPP) excitations and is observed for p-polarized light only. The incident light illuminated on top of the one dimensional metallic nano-gratings and subwavelength slits is converted into the propagating SPPs that can absorb the light efficiently in extremely thin (10-nm to more than 100-nm's thick) layers. The coupling of light to the structure in the form of the SPPs is obtained with the utility of periodicity. There are two mechanisms to produce the transmission of light in one-dimensional (1-D) metal nano-gratings with narrow slits which are the excitation of horizontal and vertical surface resonances however there is not always a clear distinction between these two ways of transferring light from the upper surface to the lower one and that their existence strongly depends on the gratings geometry. The horizontal surface resonances are cavity modes excited by the periodic structure of the nano-gratings at the grating's interfaces. Two vertical resonances existing on the slit walls can compose a fundamental waveguide mode which satisfies the Fabry-Perot condition and reflects repeatedly from both ends of the slit. Therefore, the vertical surface resonances have relations with Fabry–Perot resonances of the fundamental TM guided wave in the slits [18], and the guided modes can be excited along vertical direction, evanescent coupling mechanism accounts for this activation [19]. The responsibility of these two effects on extraordinary optical transmission (EOT) is still under debate. However, it is indicated that both mechanisms are important in the EOT [20].

Nowadays, it is clear that the real metals play a very important role in EOT, because their effect is essential for the SP excitation. The condition for the existence of the SP on a flat air-metal interface, ε'_m<-1, ε''_m<<$|\varepsilon'_m|$, is fulfilled for many metals, including the silver and gold. Concentrating the light in small areas with the assistance of extremely thin layers (plasmonic lenses), the EOT is a unique phenomenon which is introduced as the SP assisted multiple

diffractions, coupling the SPs into the aperture, and conversion back into near-field at the exit side of the aperture. The role of SP modes is essential to clarify the EOT of light through the slits. In the EOT, the aperture transmits more light than the standard aperture theory. The EOT can occur whenever some specific conditions are satisfied, i.e., the slit width must be much smaller than the incident light wavelength, the periodicity has to be in the range of wavelength and it can lead to outstanding results if the light is normally incident to the structure's surface. Subwavelength apertures have also been used to concentrate light efficiently into the deep subwavelength regions.

A considerable development has been reported for the EOT through metallic gratings with very narrow slits. The SPPs and subwavelength slits in metallic thin films are always involved with this phenomenon but the details are still under investigation [21, 23]. The SPs can be efficiently excited in the nano-structured noble metals since they almost have free-electron behavior. The noble metal nano-textured structures have special properties to produce localized regions of high energy concentration and show larger enhancement for EOT. This effect and its underlying mechanism have important applications in photolithography and near-field microscopy.

Specifically, in this chapter we present the effects of nano-grating structures on the MSM photodetector performance. Optimization of subwavelength nano-gratings shape and pitch is very much important to generate the zero-order diffraction waves. Thus, the subwavelength nano-gratings can be represented as a homogeneous medium with optical properties determined by the nano-grating geometry. When the nano-grating period is within the order of the light wavelength, the light wave may be resonant and reflects into the structure, hence the higher diffraction orders will be suppressed and resonant reflection occurs for the zero-order diffraction waves.

3. Modeling and characterization of plasmonic-based MSM-PDs

For proper design of MSM photodetector structure, it is necessary to define an appropriate model to specify the dielectric properties of the materials. In our modeling, semiconductor substrate is made up of gallium arsenide (GaAs) which is a direct band gap compound semiconductor. Usually, the GaAs substrate is preferred for the design of electronic and photonic devices, because it has unique electrical properties. Being a direct bandgap semiconductor, it can collect and emit light more efficiently than indirect band gap semiconductors such as Si and Ge. The GaAs substrate as an isotropic material has a constant refractive index of $3.666+i6.12\times10^{-2}$ in our simulation. GaAs is suitable for infrared range applications and optical fiber communication because of its wide bandgap and fast electron conduction. It also has short absorption length that enables the detector to combine wide range bandwidth with good responsivity characteristics. The GaAs has a conduction-band structure that leads to fast electron conduction.

Periodic nano-structures can produce an efficient light transmission and absorption by excitation of surface plasmons (SPs). The continuing progress in plasmonic interaction with

http://dx.doi.org/10.5772/58997

nano-structures and their outstanding effects in development of MSM-PDs design have developed a unique context for future-generation optoelectronic systems, such as, optical fiber communication systems.

The conventional MSM-PD is a symmetrical device equivalent to two back-to-back connected Schottky diodes on a semiconductor substrate. To create a Schottky junction, along with the shape and size of the interface, some essential properties, such as type and quality of metal and semiconductor must be satisfied.

A conventional MSM-PD structure is shown in Fig. 2. By impinging the light from the top on the conventional device surface, a considerable amount of illumination on top is reflected, so the light absorption inside the MSM photodetector (or substrate) is significantly reduced in device's active region. Fabrication of nano-gratings on the metal fingers of the conventional MSM-PD structure avoids this unwanted phenomenon (or light reflection), compare Fig. 2 and 3. Such nanostructure then can capture most of the reflecting light inside the active region of the device (or substrate). Hence, the individual subwavelength apertures can exhibit notable light transmission when surrounded by periodic nano-structures that harvest the externally incident light into the slit. This proposed mechanism is shown in Fig. 3.

By tailoring the electrodes structure surface with metallic nano-gratings, MSM-PDs can be modified for the light absorption and the modification process strongly depends on the corrugation parameters. Recently, different shapes of 1-D nano-structured surfaces have been developed in which noble metals, such as gold (Au) are used for nano-grating structuring. When an electric field (or a voltage) is applied between the electrodes and the device's active region is under illumination then the electric carriers (i.e., electrons and holes) are generated and drifted towards the opposite electrodes due to the electric field and can form a photocurrent. Improvement of recombination between electrons and holes can lead to enhance the light absorption in the subwavelength aperture region.

The TM polarized wave is required to excite the propagating SP waves, when the *z*-component of the light k-vector matches with the SP k-vector, because only the TM polarization has electric field component in the same direction as surface normal. The polarization is described with regard to the electric field configuration of the incident light with respect to the surface normal (angle β) as shown in Fig. 3. The wave is purely TE polarized, when $\beta=\pi/2$, and purely TM polarized, when $\beta=0$. The angle ϕ represents the direction of the plane of incidence, such that the nano-grating is in the classical mount in this model, where all the diffracted orders remain in the *x*-*z* plane and the plane of incidence is normal to the nano-grating grooves ($\phi=0$). Besides, when the grooves are parallel to the plane of incidence, the nano-grating is in the conical mount (ϕ=90). In our simulation, we used the nano-grating period of Λ=810-nm. The grating period has to be optimized to effectively couple surface plasmon resonances to the light wave and trigger the quality absorption process.

It is very important to build a new type of plasmonic-based MSM-PD with the characterization of high speed and high responsivity application which is useful in optical interconnect and communication systems. An MSM-PD speed in operation is intrinsically limited by the carrier transit time between the fingers or by the carrier recombination time. Although reducing the

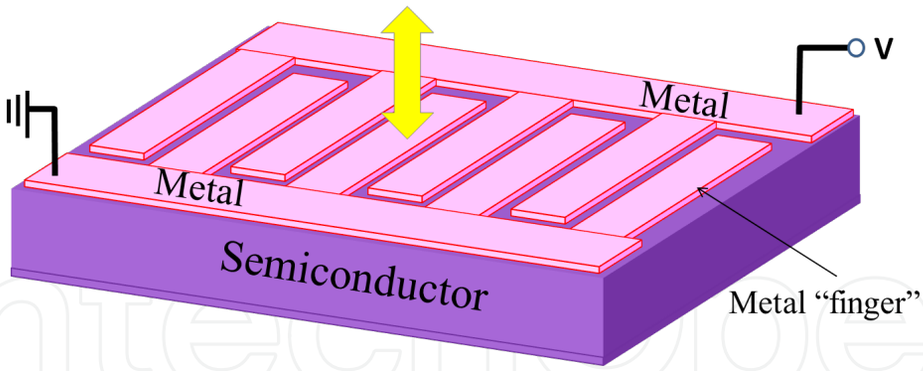

Figure 2. Schematic diagram of conventional MSM-PD structure with interdigitated electrodes (metal fingers) and semiconductor substrate (GaAs). For this symmetric device under illumination, there are undesirable light reflections.

interdigitated electrodes spacing as well as scaling down the entire MSM-PD dimensions are common ways to increase the photodetector speed, as transit time is quite small, undesirable light reflection from the surface of the electrodes and the metal fingers shadowing the detection area which leads to decreased active area, lowers the MSM-PD responsivity. Employing metal nano-gratings on interdigitated electrodes demonstrates substantial transmission enhancement through the excitation and guidance of surface plasmon polaritons into the photodetector's semiconductor region [24].

4. Plasmonic-based MSM-PD simulation model

Metallic nano-grating structures produce efficient and ultrafast photodetection properties. In this section, a plasmonic-based MSM-PD is introduced which utilizes electromagnetic and optical properties of nanostructures to enhance the light harvesting inside the device active region. The plasmonic-based MSM-PD consists of a semiconductor absorbing layer on which the interdigitated electrodes have been deposited to form two back-to-back connected Schottky diodes. The interdigitated electrodes are designed to resolve the conventional MSM-PD's degraded efficiency problem because of the metallic electrodes opacity. Also, the MSM-PDs are patterned by nano-gratings to improve the light capturing capacity into the device active region. Electromagnetic fields coupled to a charge density wave propagating at the metal-dielectric interface produce transverse-magnetic optical surface waves namely surface plasmon polaritons. The coupling condition for the SPPs is provided by metallic nano-gratings with optimized dimensions and geometry. This structure has the feasibility to create a plasmonic lens which utilizes plasmonic effects to produce surface plasmon resonances and funnel the energy toward the central focal point.

The design of high performance plasmonic-based MSM-PD is shown in Fig. 3. A plasmonic-based MSM-PD structure has three separate regions or parts, namely, the incident region (the metal nano-gratings), the under layer and the subwavelength slit region, and the transmission region (the semiconductor substrate). The nano-scale gaps between the interdigitated electro-

http://dx.doi.org/10.5772/58997

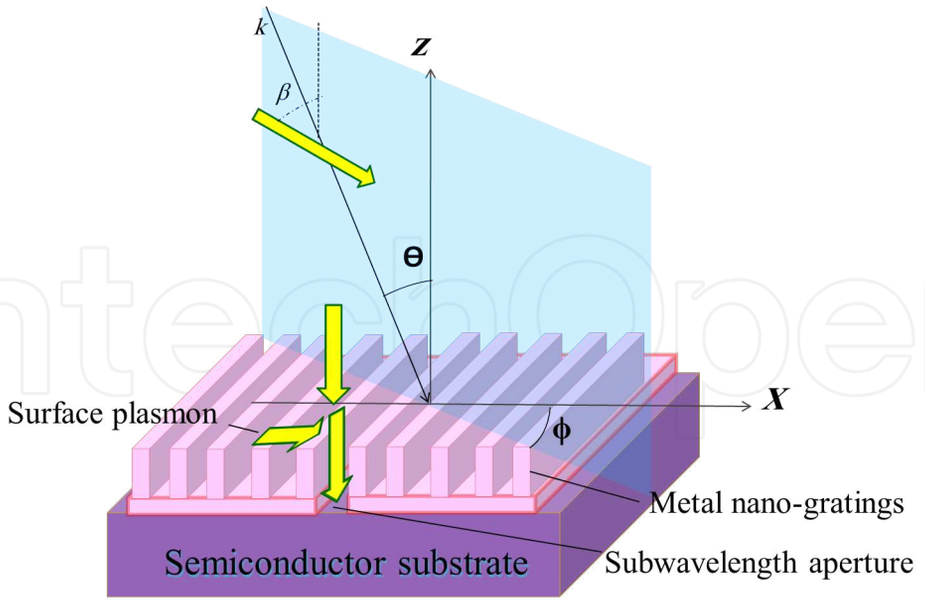

Figure 3. Schematic diagram of MSM-PD structure with rectangular shaped nano-gratings on top of the subwavelength slit. The subwavelength slit layer is just on top of the semiconductor (GaAs) substrates. The excited SPPs travel along the interface to reach the subwavelength slit/aperture.

des in the MSM-PDs result in a huge increase in bandwidth and reduction in dark current, whereas the conventional pin photodetectors with similar sized active areas are unable to achieve that amount of light absorption.

In addition, the near-field characteristics and associated field enhancements can be achieved for periodic nano-structures and subwavelength apertures with aid of the SPPs interactions. This suggests that, properly designed metallic nano-grating grooves trigger surface plasmon polaritons under illumination and carry them toward the central slit. By using a subwavelength central slit, a well-directed source of light could be generated, an exciting development that is being pursued as a source for a variety of optical technologies. The light continuously re-emits from a very small area surrounding the central aperture which is associated with properties of the Fabry-Perot cavity resonances for symmetric SPP modes of the slit. Particularly, The SPPs which are supported by the active region of the device show a great potential of subwavelength photonic phenomenon. The excitation of the SPP waves causes a resonance absorption, which can be observed as partial or total absorption of the incident light. The absorption enhancement caused by the excitation of SPPs is associated with the incident photons and their interaction with the nano-gratings, while Fabry-Perot like resonances are included in transmission absorption process through the subwavelength slits.

In periodic subwavelength structures, the nano-gratings are deposited on top of the under layer from the same metal (such as gold). The absorption enhancement can be achieved by the SPP resonant excitations in the subwavelength region. Here, the FDTD method is used to specify the TM polarized plane wave via Poynting vector. The SPPs are evanescent waves, which are generated by the interaction between the surface electron densities and the electromagnetic fields whilst trapping the light power inside the surface. Since the SP modes have

longer wave vectors than the light waves with the same energy, the SP waves are non-radiative on smooth metallic surfaces and cannot propagate in non-metallic media. One way to excite the SPPs is the nano-grating coupling technique in which the incident radiation is coupled into the SPPs using periodic surface corrugations with proper dimensions. The nano-grating grooves are perpendicular to the x-direction and its dimensions and geometry are optimized to couple the light near the design wavelength, that is, providing the missing momentum in order to make the SPPs propagate along the z-direction. In a metal-dielectric interface, the SPP wave vector matching condition for a metal nano-grating can be defined with some changes to the well-known prism resonance condition. Hence, in a metal-dielectric interface, the SPP propagating constant or wave vector matching condition for a metal nano-grating with the period of Λ is given by [22, 24]:

$$k_{spp} = \frac{\omega}{c}\sin(\theta) \pm \frac{2\pi l}{\Lambda} = \frac{\omega}{c}\sqrt{\frac{\varepsilon'_m \varepsilon_d}{\varepsilon'_m + \varepsilon_d}} \tag{5}$$

where, ω is the angular frequency of the incident light wave, c is the speed of light in vacuum. l is an integer number i.e., l=1, 2, 3, …, N and θ is the light angle of incidence to the device normal. This relation illustrates that the wave vector of a given frequency is smaller than the SPP wave vector, therefore the light wave vector should increase with the support of a coupling mechanism to provide SPPs which in this case is satisfied by nano-grating structures.

The wave vector has to be complex as the metal permittivity is complex, $\varepsilon_m = \varepsilon'_m + i\varepsilon''_m$. To trigger SPPs, the dielectric permittivity has to change sign in the metal-dielectric interface. The values of dielectric constant vary for different frequency ranges. To represent the influence of electric field in organizing electric charges and dipoles in the medium, we introduce electric displacement field, $D=\varepsilon_0\varepsilon_r E$, between two isotropic media where, ε_0 is the vacuum permittivity and ε_r is the relative (dielectric) permittivity. Here, the real part of complex dielectric permittivity of gold is used. The dielectric permittivity of air as the incidence medium is denoted as ε_d. The electric displacement field derived from the Maxwell's equation is continuous across the interface. With the continuous normal component of D across the interface and the permittivity sign difference for metal and dielectric, the electric field changes direction passing through two different media. This characteristic will only be satisfied if there is a normal component for electric field across two regions that is TM polarization.

We are interested in metals with the large negative real part and a very small imaginary contribution to the dielectric constant for the design wavelength, such as gold. The SPP damping while propagating along the interface will be determined by the imaginary part of the wave vector parallel component. As the researchers demonstrated their results for noble metals, such as gold and silver in metal-dielectric interface, there will be a high field confinement at the interface while the losses remain minimum. When the plasmonic excitations occur, the left side of equation (5) matches the wave vector of the excited SPP (k_{spp}), that is the equivalence of the interaction of incident radiation and l_{th} diffracted order with the wave vector of the SP at the interface.

http://dx.doi.org/10.5772/58997

The FDTD as a powerful engineering tool allows for the effective and powerful simulation and analysis of sub-micron devices with very fine structural details. The FDTD algorithm was originally proposed by K. S. Yee in 1966 [25]. In order to investigate the optical response of plasmonic-based MSM-PD, finite difference time-domain (FDTD) numerical method is used as a premier solution for the simulation of propagating electromagnetic field by solving Maxwell's curl equations in time domain. The computational mesh points (grids) are made up of unit cells, and the electric (E) and magnetic (H) fields are arranged at special places of the computational domain denoted by (i, j, k) with respect to Ampere and Faraday's laws. The FDTD method is able to model light propagation, scattering, diffraction, reflection, and polarization effects.

The Opti-FDTD software package developed by Optiwave Inc. was used to perform a 2D simulation, and it is the first software to employ the Lorentz–Drude model into the FDTD algorithm to calculate the transmission and reflection spectra. The FDTD simulation results have demonstrated significant light-capture performance through periodic 1-D slit arrays, which is useful for the design of ultrafast MSM-PDs.

In this model, the light wave hits on the nano-grating structures perpendicularly and passes through the subwavelength aperture and finally reaches to the semiconductor substrate.

This chapter's focus is on nano-gratings architectures that can increase the MSM-PD responsivity by exciting the SPPs and manipulation of light in the subwavelength slit. It has been reported that the rectangular nano-gratings produce the best absorption process, however, we will present some new more qualified nano-gratings with more efficient performance. The most influential parameters controlling the device light absorption can be categorized in two general groups. One can be the basic structural differences for nano-gratings clearly distinguishable with respect to their cross sections such as nano-gratings shape and dimensions, metal nano-grating heights, duty cycle, and number of nano-gratings on each side of the central slit. The other one is optimization process for subwavelength aperture region as subwavelength slit width, and electrodes (under layer) thickness. Furthermore the incident light polarization and angle of incidence play an important role to produce quality light absorption in optimized plasmonic-based MSM-PD. To verify the importance of these features, the power flow through the central subwavelength slit for plasmonic-based MSM-PD is compared with the amount of power reaching the active region for conventional MSM-PD. Improved light interaction process with different nano-grating shapes and geometries results in verification of the simulated results for the design and development of high responsivity MSM-PDs which have applications in high-speed optical fiber communication, high-speed sampling, and chip to chip interconnectors. The light absorption enhancement factor (LAEF) is introduced as a dimensionless quantity to measure the optimal absorbed radiation ratio to the whole incident power [26]. Therefore the impact of nano-gratings implementation on the quality of light flux transmitted into the active region of the MSM-PD is well approved compared with the conventional MSM-PD without the nano-gratings.

5. Simulation results and discussion

5.1. Electric field distribution inside the GaAs substrate

In this subsection, local electric field intensity distribution for conventional and plasmonic-based MSM-PD structures will be clarified through simulations to evaluate the adequacy of plasmonic-based structure. We use a custom designed Matlab code to show the density plot and the transmitted power into the substrate for two different structures. While the radiation reaches to the structure normally, Fig. 4(a) represents the electric field distribution in a conventional device without nano-gratings but with the Au contacts just on the GaAs substrate. The slit width is 100-nm and the under layer height is 60-nm. Therefore, in this situation, the light transmission inside the substrate is not influenced by the surface plasmon excitations and the incident light normally passes through the subwavelength aperture. Different colors represent each point's electric field strength in the density plots. Also, rectangular nano-grating structures are designed and deposited on the metal contacts to take the plasmonic effects into account. Fig. 4(b) demonstrates the electric field confinement in the GaAs substrate at cross section of plasmonic-based MSM photodetector device and the field concentration is due to SPP coupling with nano-structures. The maximum intensity appears for the part of the substrate located just under the slit [27].

Due to the plasmonic interactions and the confinement of light into the central subwavelength slit, it is obvious from Fig. 4 that the grating assisted MSM-PD tendency is to concentrate the power (or energy) into the photoactive region which is just below the central slit. Therefore, implementation of the nano-gratings enables the photodetector to lead the light into the central aperture quite effectively. Hence, it is important to obtain optimized geometrical parameters for efficient light confinement, and it is what we describe in the following subsections.

5.2. Effect of duty cycles on the LAEF

For 2 similar nano-gratings with the discrepancy in profile shapes, the light harvesting ability can be different. The Au nano-grating profile and geometry on the GaAs substrate can make changes in the absorption enhancement spectrum. Therefore it is interesting to discuss the effects of duty cycle on the LAEF of the nano-structured MSM-PDs. Duty cycle (DC) of corrugations is the percentage of ridges width to the nano-grating period, i. e. 60% DC refers to the ratio of the nano-gratings grooves width to the ridges width of six to four in one period. We specify the optimum duty cycle for trapezoidal and rectangular-shaped nano-grating profiles which are designed with optimum heights [28].

Under normal incidence, the LAEF spectra in rectangular-shaped nano-grating structures is calculated for different duty cycles, such as from 30% to 100%, as shown in Fig. 5, while the subwavelength aperture width has been kept constant at 50-nm, the under layer thickness and the nano-grating height were 20-nm and 120-nm, respectively. It can be inferred that the peak wavelength is different for each specific duty cycle and the maximum LAEF, with the amount of ~32.7, occurs for 40% duty cycle. It is clear that the duty cycle can affect the peak wavelength as well as the amount of light flux transmitted into the active area of the MSM-PDs.

http://dx.doi.org/10.5772/58997

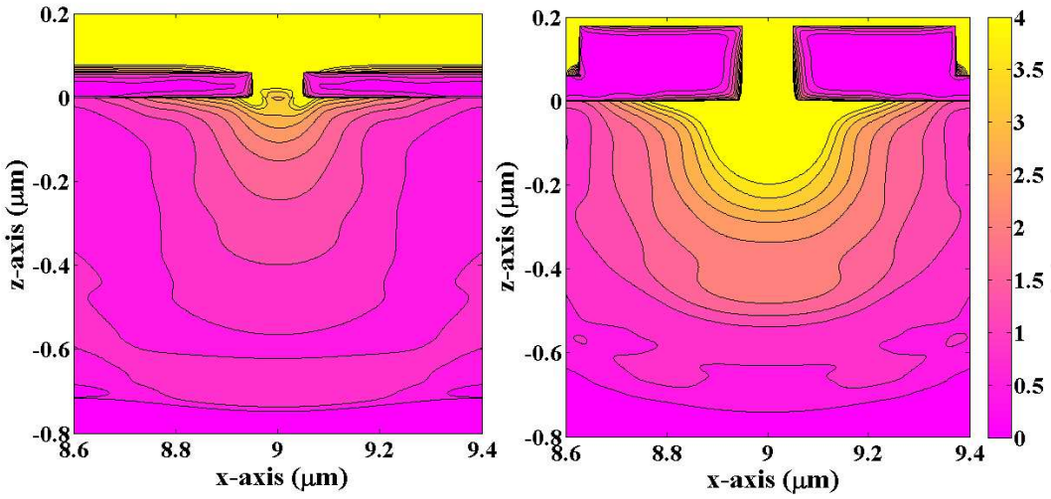

Figure 4. Field distribution at the cross section (a) conventional MSM-PD, (b) rectangular plasmonic-based MSM photodetector. The calculated total electric field intensity distribution inside the GaAs substrate is shown using the following parameters: the subwavelength slit width of 100-nm, gold under layer thickness of 60-nm, and the nano-gratings height of 100-nm for (b).

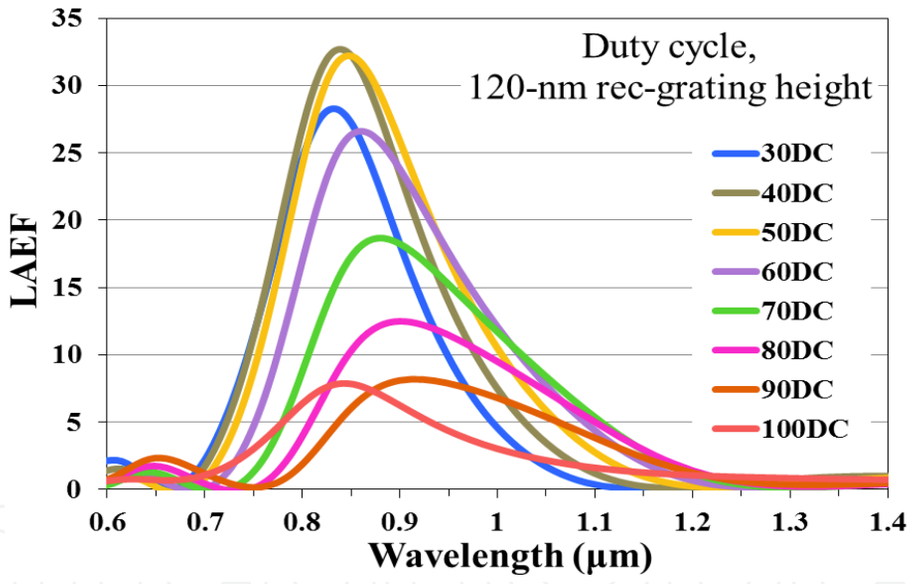

Figure 5. Light absorption enhancement factor spectra of MSM-PDs with rectangular-shaped nano-gratings for various duty cycles ranging from 30% to 100%.

The optimum duty cycle has also been specified for trapezoidal-shaped nano-grating profile with the subwavelength aperture width and under layer thickness of 50-nm and 20-nm, respectively. In this case, the maximum LAEF is obtained~31.5 for 40% DC which is the same duty cycle as the optimum DC for rectangular-shaped nano-gratings.

The results shown in Figs. 5 and 6 illustrate that the amount of LAEF is a function of duty cycle which grows gradually towards the 40% DC and drops down dramatically towards higher DCs and the peak wavelengths are also red-shifted for the LAEF curves of the higher duty

cycles for both the structures. In the case of the rectangular and trapezoidal nano-grating profiles designed with their optimum nano-grating height, we can infer that the amount of light transmitted into the active region not only depends on the nano-gratings height and shape but also on the amount of duty cycles. Besides, for rectangular-shaped nano-grating profile shown in Fig. 5, 100% DC indicates that the whole structure is like a conventional MSM-PD having a thick under layer with height of about 140-nm, the resulting thickness is the sum of under layer thickness and the nano-grating height, while for trapezoidal shaped nano-gratings, there will be triangular grooves between the trapezoidal ridges for 100% DC, Fig. 7.

5.3. Impact of subwavelength aperture width on the LAEF

We discuss the impact of subwavelength aperture width on the light absorption and reflection for MSM-PDs and the results are discussed for different duty cycles. Compared with the incident light wavelength (λ_0), the aperture width is very small, hence only symmetric and fundamental SP modes will propagate into the slit. When the subwavelength slit width is much smaller than the incident light wavelength (λ_0), in addition to the light transmission and absorption caused by manipulation of metal nano-gratings, the light harvesting and confinement in the semiconductor substrate can be obtained via optimization of subwavelength aperture. Fig. 8 shows the simulation results of the absorption spectrum for several subwavelength aperture widths when the number of nano-gratings on each side of the slit (subwavelength aperture) is 9, and the nano-grating period and the nano-grating height are kept constant at 810-nm, and 100-nm, respectively. However, a portion of the lights is reflected in the central slit area, as shown in Fig. 9. The interesting point is that the range of wavelengths in the spectrum corresponding to the minimum reflection for the LRF curves in Fig. 9 is equivalent to the range of maximum LAEF for the same structure.

The results for less than 50-nm and more than 500-nm width slits are not presented here because the LAEF is reduced for very thin and very wide slits. The optimized slit width is selected as 50-nm which is much easier to fabricate compared with thinner slits and shows very promising results to improve the device performance.

The simulated results show that the LAEF decreases rapidly with the increase of the subwavelength aperture width from 500-nm to 50-nm. Figure 8 shows clearly that the LAEF is more than 12-times with 50% DC and about 13.5-times with 60% DC for a 50-nm subwavelength aperture width, the narrowest slit in this simulation, also with presentation of LAEF curves for 40% and 70% DCs of the aforementioned slit width, we show that 60% DC is optimized for this special structure. However, the LAEF is ~4-times with 50% DC but a little lower with 60 DC for a slit width of 250-nm and the LAEF wavelength is red shifted for all bigger DC.

The effective refractive index is a function of slit width for symmetrical SP modes when the slit experiences the TM incident wave. Therefore, with reducing the subwavelength aperture width, the effective refractive index increases and leads to an enhancement of the light absorption inside the active region.

http://dx.doi.org/10.5772/58997

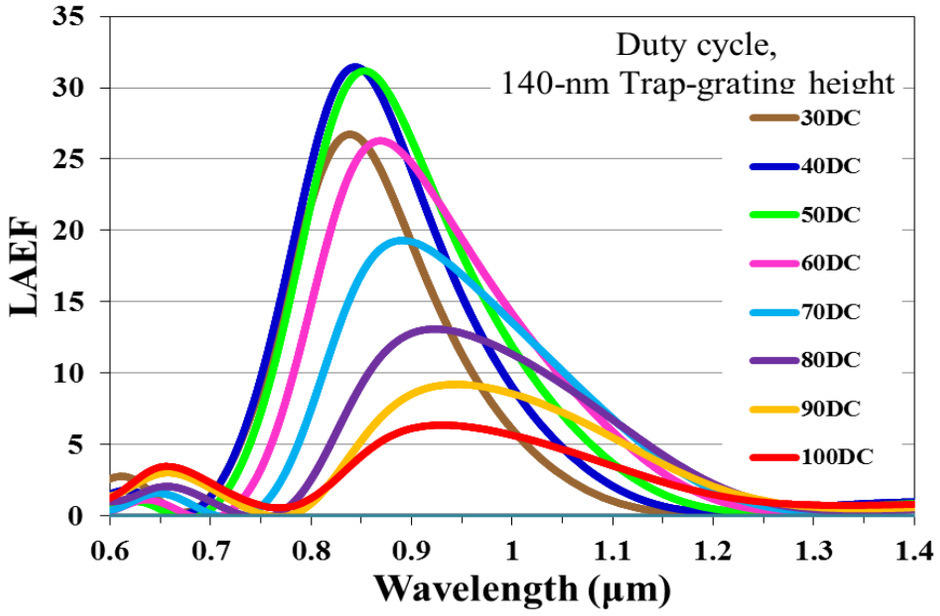

Figure 6. Light absorption enhancement factor spectra of MSM-PDs with trapezoidal-shaped nano-gratings for various duty cycles ranging from 30% to 100%.

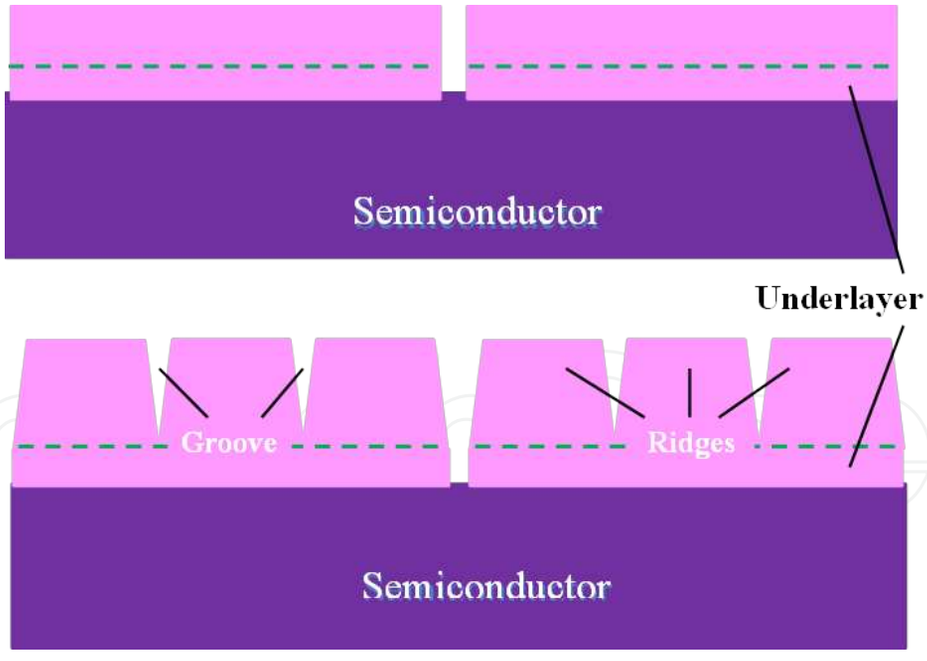

Figure 7. Cross-section of rectangular and trapezoidal-shaped nano-gratings while the duty cycle is 100%.

However, the idea for optimization of the MSM-PDs can be made more precisely by modifying the amount of transmitted light power through the subwavelength slit in the GaAs substrate [29]. Therefore, at normal incidence, we made this amendment by the subtractions of localized

power near the top of the substrate and the power propagating to the bottom of the substrate, that is the LAEF values at the slit opening and beyond the slit opening at the outer edge of the substrate. The subtracted amount for LAEF is presented in Fig. 10 for the optimized geometry presented in Fig. 8, that is 50-nm slit width, 60% duty cycle. The maximum LAEF is almost unchanged and the fact that a minor amount of energy is lost from the substrate is justified as long as the device dimensions are optimized. Also the absolute values for Poynting vector in x direction are presented for 3 depths of the GaAs substrate, top, 0.1 μm from top and bottom. The $|S_x|$ value is negligible at the bottom of the substrate compared with the slit opening.

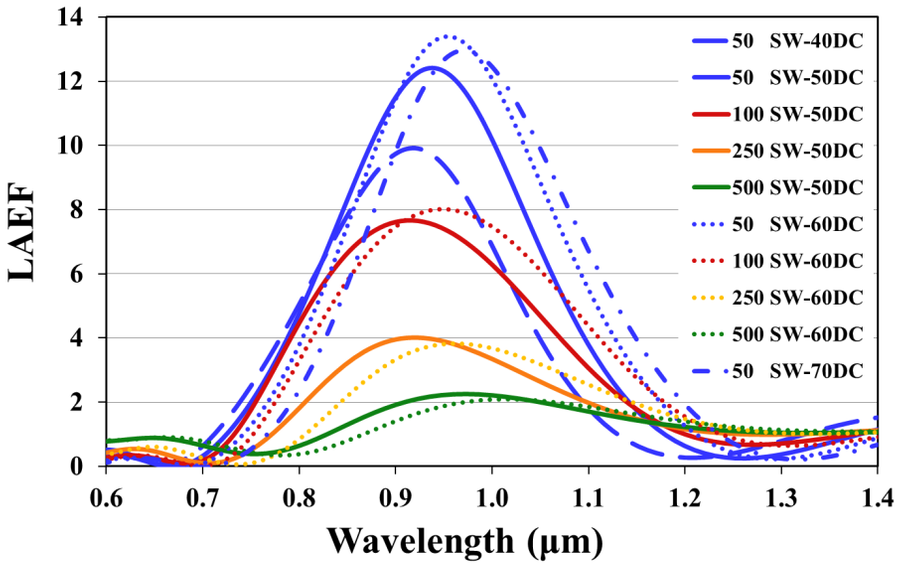

Figure 8. Light absorption enhancement factor spectra of MSM-PDs with rectangular-shaped nano-gratings. Different curves show the effect of slit width (SW) and duty cycle (DC) variations on the LAEF. Here, the under layer thickness and nano-gratings height are kept constant at 60-nm and 100-nm, respectively.

5.4. Impact of incident angle on LAEF curves

We present some results to investigate the effects of incidence angle upon the maximum LAEF for plasmonic-based MSM-PD device. The incident angle varies through a straight angle with negative and positive values, ranging from-90° to 90°, representing inclination from the normal incidence to left and right, respectively. While changing the angle of incidence for illuminated light in simulation, we show the device's most efficient light absorption enhancement for a specific angle. Fig. 11 shows maximum LAEF curve for various incident angles for the nano-grating structures with the subwavelength slit width of 50-nm and nano-grating height of 100-nm while the DC is kept constant at 60%, they are the parameters for the optimized curve producing the maximum LAEF in Fig. 8. The resonant wavelength is constant for most of the angles at 947-nm. The presented results indicate that the optimized incident angle is-46° for this geometry.

http://dx.doi.org/10.5772/58997

5.5. Nano-grating height optimization in plasmonic-based MSM-PD

With the variation of nano-gratings height, different sets of results show significant changes in the amount of light transmitted into the active area of the MSM-PD. Hence the height of the ridge is an effective parameter in optimization of the detector performance [30]. We present the simulation results for rectangular and trapezoidal MSM-PDs with different nano-grating heights. The incident light with TM polarization was perpendicularly illuminated on the groove profiles and we have calculated the amount of light flux transmitted into the slit for four different heights in rectangular and trapezoidal nano-grating assisted MSM-PDs.

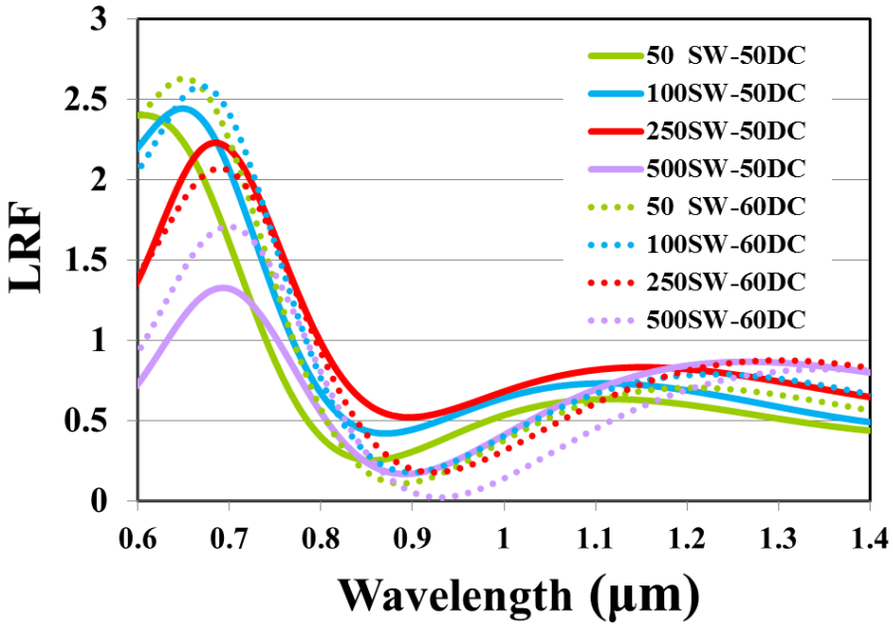

Figure 9. Light reflection factor spectra of MSM-PDs with rectangular-shaped nano-gratings. Different curves show the effect of slit width (SW) and duty cycle (DC) variations on the Light reflection factor.

Figure 12 shows the LAEF spectrum for different heights of the rectangular shaped nano-gratings in plasmonic-based MSM-PD, such as 80, 100, 120, 140-nm. Simulation results confirm that 120-nm is the optimized height for this design. The peak wavelength behaves like a sinusoidal manner and wavelength (λ) is red shifted as the ridge's height increases. The duty cycle is 60% while the subwavelength aperture width, and subwavelength aperture thickness are kept constant at 50-nm, and 20-nm, respectively. There are some interpretations to analyze the curves. The SPPs coupling process and the following expected absorption can easily occur for higher gratings and reduces after certain heights. This light absorption has a maximum for a specific wavelength in the spectra which varies in different heights, and for the wavelengths higher than the peak, the amount of LAEF decreases because the incident light might be coupled into radiative SPs rather than bound SP modes.

Also, several sets of numerical analysis are carried out to illustrate the effect of trapezoidal-shaped nano-gratings on the optimized height at which the maximum resonance transmission occurs. The simulations are performed for 4 different nano-grating heights of 100, 120, 140, and 160-nm with the subwavelength aperture width of 50-nm and the under layer thickness of 20-nm. The results are shown in Fig. 13. The LAEF is 26.3 times in its maximum for the curve representing the 140-nm nano-grating height for the duty cycle of 60%.

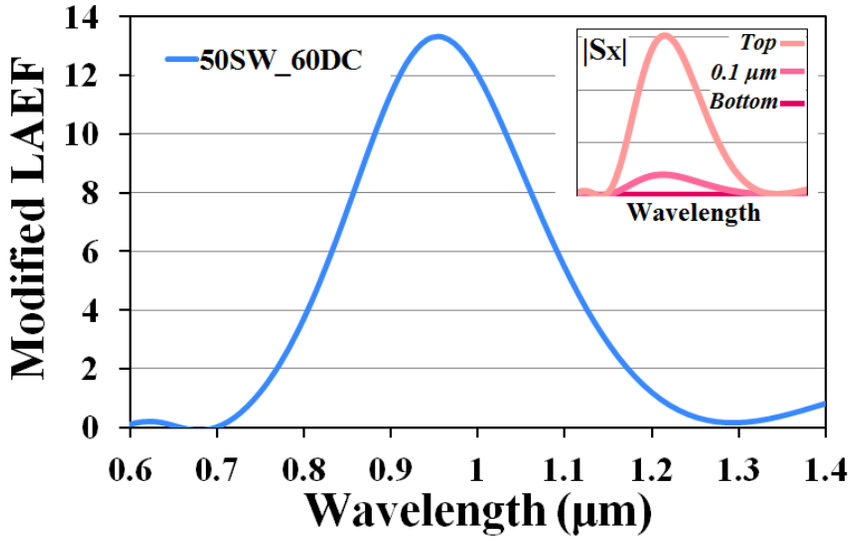

Figure 10. Modified LAEF for plasmonic-based MSM-PDs with 50-nm slit width, 100-nm nano-grating height, and 60% duty cycle. The inset represents the absolute value of S_x in different depths of GaAs substrate, the top, 0.1 μm depth from the substrate surface, and the bottom.

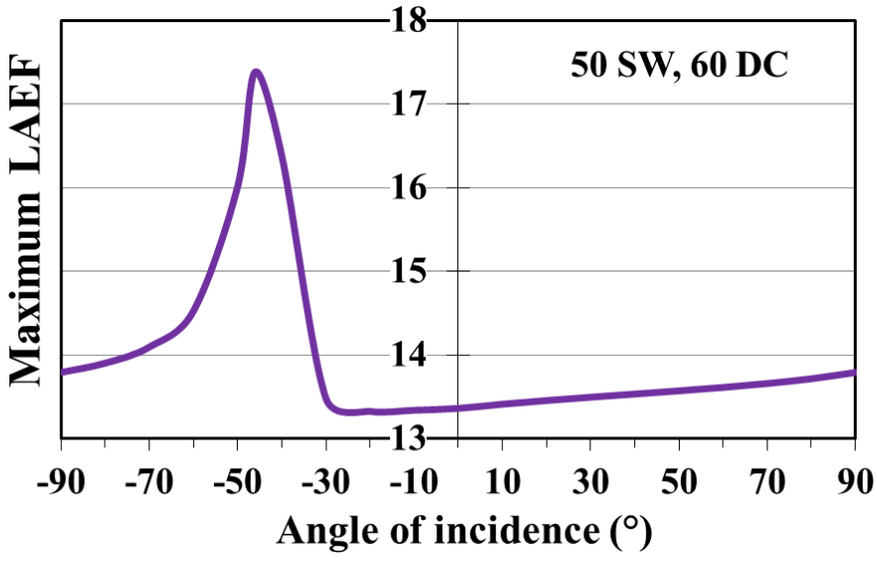

Figure 11. Maximum LAEF versus incidence angle characteristics for MSM-PDs with 50-nm slit width and 60% DC. Here, the subwavelength aperture height and nano-gratings height are kept constant at 60-nm and 100-nm, respectively.

http://dx.doi.org/10.5772/58997

From Figs. 12 and 13, it can be recognized that the optimum wavelength is red shifted for higher nano-gratings in both figures. However, trapezoidal nano-gratings height at maximum light absorption, 140-nm, is higher than the optimum height of its rectangular counterpart, 120-nm, while its resonant wavelength is blue shifted.

5.6. Nano-grating geometries effect in plasmonic-based MSM-PD

There is no doubt about the effects of nano-grating textured structures and geometries on light trapping inside the device active region as they are responsible for the creation of the SPPs which can assist for the light confinement in the subwavelength regions. Hence we analyze the MSM-PD device performance and its enhanced responsivity for different nano-grating shapes.

By involving plasmonics (i.e., metallic nano-gratings), the device performance has been improved due to the advances in nano-technology fabrication methods. Focused ion beam (FIB) lithography, electron beam (E-beam) lithography, and nano-lithography are the new approaches to fabricate nano-scale devices. These techniques can be used to obtain the state-of-the-art for very small nano-structures in order of tens of nano-meters which are the accepted dimension for visible and near infrared regions [31].

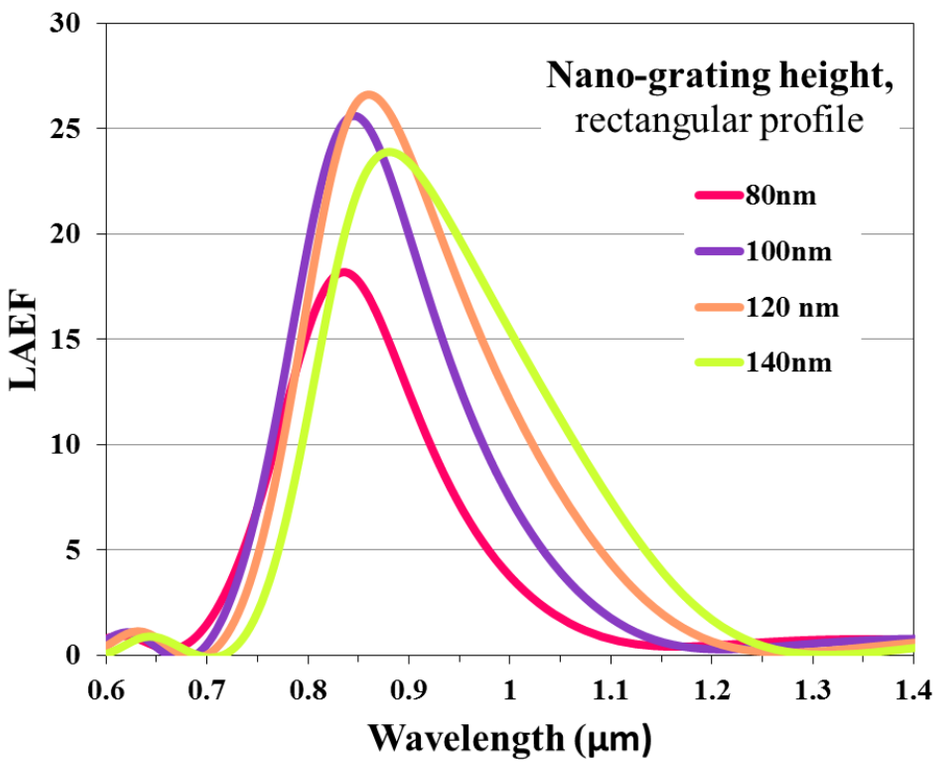

Figure 12. Light absorption enhancement factor spectra of the rectangular nano-gratings with different heights. Here, DC is 60% and subwavelength aperture width is 50-nm.

In general, a good light absorption performance is achieved for rectangular-shaped nano-gratings. It has been proved that the rectangular nano-gratings are the best option for the design of nano-gratings to improve the MSM-PDs performance. The normal wall nano-gratings are easily fabricated with lithography and etching, while in focused-ion beam (FIB) milling, the nano-gratings are rather taper than the rectangular one. The observation of scanning electron microscopy images represents the nano-gratings with taper walls rather than the rectangular nano-gratings. The metallic nano-gratings fabrication is not an easy process but the FIB lithography is an approved technique to develop elaborate structures with the nano-gratings. This nano-scale fabrication technology is very promising to access near field excitations and detection of the plasmon polaritons at air/Au interface.

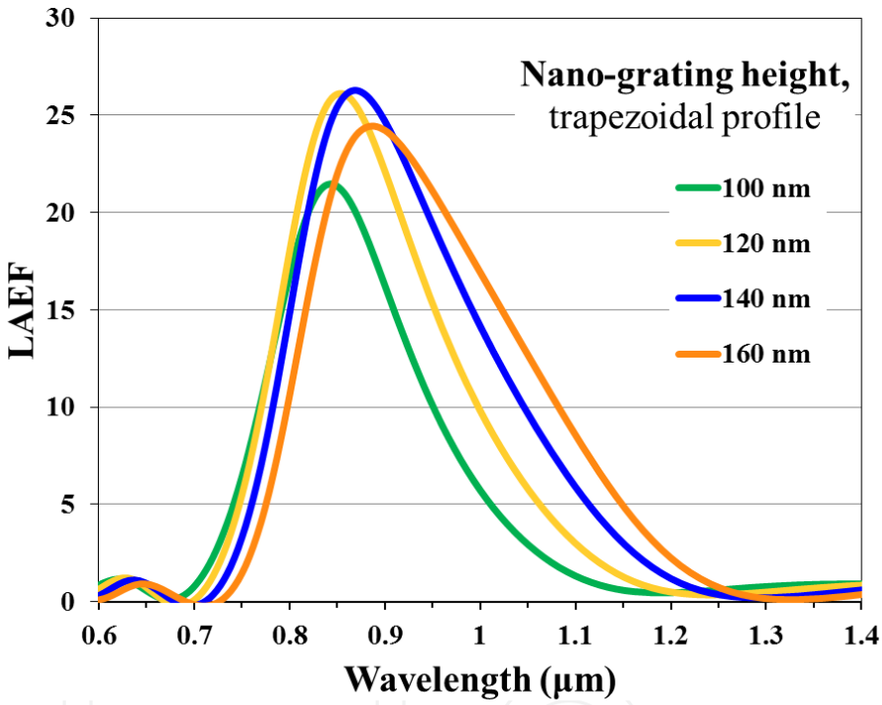

Figure 13. Light absorption enhancement factor spectra of the trapezoidal profile nano-gratings with different heights. Here, DC is 60% and subwavelength aperture width is 50-nm.

Here the plasmonic-based MSM-PD structures are set with the rectangular, trapezoidal, and ellipse-wall nano-grating profiles and their behaviors are compared with each other. It has been reported that the straight wall nano-gratings produce an optimum light absorption for plasmonic-based MSM-PDs, but under practical device manufacturing situations, the rectangular shaped profile is closer in appearance to semi-trapezoidal nano-gratings. Then we introduce and characterize grating-assisted MSM-PD which utilizes ellipse-wall nano-gratings and prove that it achieves better efficiency than rectangular and trapezoidal counterpart.

http://dx.doi.org/10.5772/58997

Metallic nano-grating geometries affect the LAEF in MSM-PDs. Figure 14 shows the light absorption enhancement spectra evolution for MSM-PDs with triangular, rectangular, trapezoidal with 0.4, 0.5, 0.8, and 0.9 aspect ratios, and the ellipse-wall nano-gratings with 0.5, and 0.9 aspect ratios. Aspect ratio (AR) is introduced to define a relationship between the width of upper and lower bases for taper and ellipse wall structures as a dimensionless coefficient smaller than unity. For ordinary structures, the lower base and for inverted ones the upper base is always bigger. These groove shapes along with the differences between their aspect ratios are shown in Fig. 15. The simulation results illustrate a strong confinement for the rectangular shaped structures, although the realistic subwavelength nano-gratings do not have the normal walls. The maximum LAEF for taper and rectangular profiles are quite close.

However, we introduce a novel grating structure for our design with ellipse walls which has recently been stated to have more light capturing efficiency than the rectangular and taper nano-grating profiles [32]. As stated the experimental results in [31], the analysis of atomic force microscope (AFM) systems and scanning electron microscope (SEM) images demonstrated the trapezoidal structures rather with curved walls than the linear walls.

Therefore, we have designed the ellipse-wall nano-gratings with legs satisfying the exponential equation having an exponential coefficient of 0.5. The exponential coefficient is supposed to satisfy the exponential function of $z=C\ e^{x}$ for nano-gratings lateral walls, where C is the exponential coefficient. Performing the simulations on these ellipse-wall nano-structures gives a better view of more realistic condition for nano-scale devices. The simulation is performed for the under layer thickness of 20-nm, the nano-grating height of 120-nm, and the subwavelength aperture width of 50-nm which are optimized values for a MSM-PD with rectangular symmetric nano-gratings [33].

Besides, the results of light absorption for trapezoidal structures with different aspect ratios are presented. In the case of slanted walls, the increase of slit opening width is a drawback for reflection of gap plasmon from the upper termination resulting in a weak LAEF, because the cavity nature which is responsible for resonant absorption faded away with variation of the slit opening width. However, the decrease of taper aspect ratio leads to a blue shift resonance position. Figure 14 shows this slight blue shift while this parameter changes from 0.9 to 0.4 for tapered nano-grating structures.

As shown in Fig. 14, the plasmonic interactions are more efficient for ellipse wall nano-gratings. We know that the localization of optical energy around sharp corners is remarkable. The nonlinear design of ellipse-wall nano-gratings enables the possibility to improve energy concentration in the active region of the MSM-PD device because the energy flow is facilitated through the interface in comparison with the rectangular nano-gratings. Depending on the aspect ratio parameter, that is the normalized value of bottom side to the top side width as shown in Fig. 15, nano-gratings can increase their LAEF. Ellipse-wall nano-gratings improve their performance from LAEF of 20 (for 0.5 aspect ratio) to 28 (for 0.9 aspect ratio). Even the maximum LAEF of rectangular nano-grating, 26.5, is less than 0.9 aspect ratio ellipse-wall structures. In addition, the maximum peak wavelength is red shifted for rectangular structure. While the 0.9

aspect ratio ellipse-wall nano-grating is the most suitable structure in light absorption, it is worth noting that the 0.5 aspect ratio ellipse-wall nano-gratings offer a better transmission in comparison to their trapezoidal counterparts. They almost doubled their efficiency compared with the 0.5 aspect ratio taper profiles from 10.5 to 20.3.

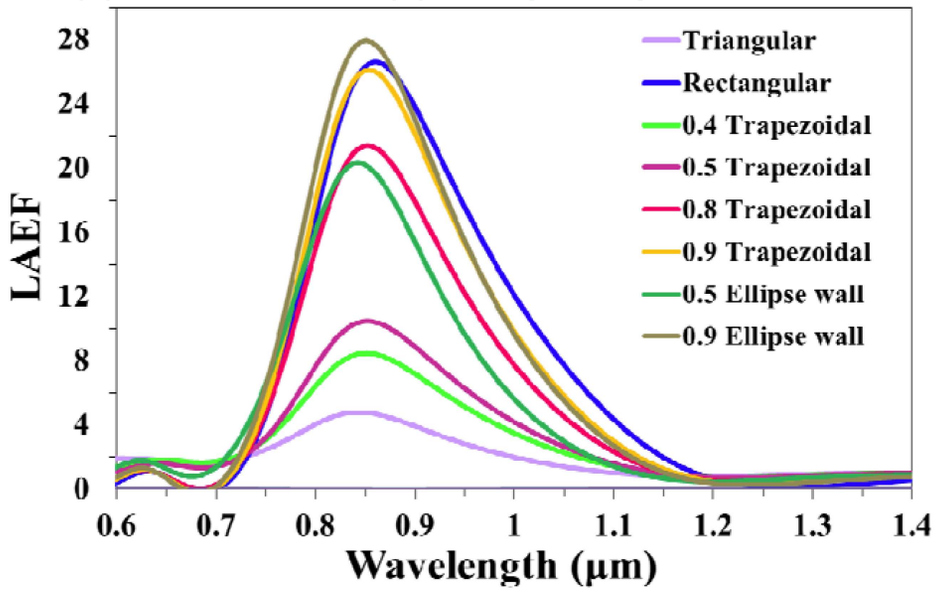

Figure 14. Light absorption enhancement factor spectra of MSM-PD with triangular, rectangular, taper nano-grating structures with 0.4, 0.5, 0.8, and 0.9 aspect ratios, and ellipse wall nano-gratings with 0.5 and 0.9 aspect ratio and exponential coefficient of+5. The duty cycle of corrugations, subwavelength aperture thickness, and the nano-gratings thickness are 60%, 20-nm, and 120-nm, respectively.

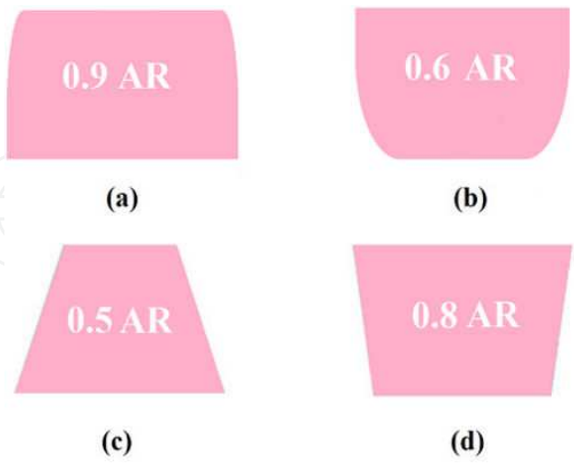

Figure 15. Ellipse-wall nano-gratings with the aspect ratio (AR) value of 0.9 and 0.6 for (a) and (b), respectively. For (a) and (b), the lateral walls are function of exponential equation with the exponential coefficient of+5 for (a) and-5 for (b). (c) and (d) are taper (trapezoidal) and inverted trapezoidal structures with 0.5 and 0.8 aspect ratios. For inverted structure, the lower base is bigger. The aspect ratio defines a relationship between two parallel bases widths of trapezoidal and ellipse-wall nano-gratings.

http://dx.doi.org/10.5772/58997

5.7. Impact of under layer thickness

Here, we discuss the impact of under layer or subwavelength aperture thickness (Uth) on the amount of transmitted light through the active region of the MSM-PD. Under layers are the photodetector's metallic electrodes which metallic nano-gratings can be designed on them. Optimization of this parameter also affects the light absorption enhancement in the MSM-PDs. The thick under layers absorb a proper amount of the incident lights and the carrier recombination become more prominent which reduces the internal quantum efficiency. The thinner under layer leads to better electrical properties moreover they have advantages of material saving and higher carrier collection efficiency; however they lose light harvesting proficiency which can be resolved by implementation of nano-grating structures of the same metal. The reduction of the under layer thickness enhances the LAEF, because in this case the EOT can also occur in the flanked slits other than the central aperture. Here, the under layer thickness attenuation effect is shown, which assists the light absorption in the device in addition to the light absorption enhancement caused by optimization of other parameters, i.e. nano-gratings shape. As expected, an ideal rectangular nano-grating shape with the thinnest under layer contributes more effectively in the light absorption in comparison to the thicker under layer heights. However, the amount of LAEF for ellipse wall structure is higher than the rectangular grooves, because in this design, the central slit opening has no corner which avoids useless light confinement at sharp edges, also the slit opening is broader, so there is less reflection for the illuminated light at the top due to the grooves' non-linear walls and a greater part of the energy involves in the SPP coupling at metal-air interface. Design of the nano-gratings with the thickness of 120-nm, which is the optimized height for rectangular nano-grating as shown in Fig. 12, results in about 32.8 fold enhancement for ellipse-wall nano-gratings with 0.9 aspect ratio and exponential coefficient of 0.5 when the duty cycle is fixed at 40% and the subwavelength slit width is 50-nm, but ellipse-wall nano-gratings quite close absorption peak to rectangular nano-grating with the height of 120-nm is the result of doing simulations for optimized rectangular nano-grating.

While absorption is enhanced for thinner under layers, useful results will be revealed through comparison of absorption curves for optimized nano-grating thickness of ellipse-wall nano-gratings and rectangular nano-gratings, 140-nm and 120-nm, respectively. Our simulated results indicate better enhancement of LAEF for ellipse-wall nano-gratings with optimized thickness of 140-nm that is 33.6 compared with maximum LAEF of 120-nm rectangular nano-grating which is 32.7. These results are shown in Fig. 16.

In addition to the influence of under layer thickness on the amount of transmitted light flux into the device active region, we can also demonstrate under layer's direct influence on other structural parameters like duty cycle. Looking back at sections 5.2 and 5.3, we notice the LAEF curves calculated in different duty cycles. In Fig. 8, for the slit widths of 50-nm, the 60% is the optimized duty cycle while in Fig. 5 and 6, the optimized duty cycle is 40%. We mentioned this to prove the fact that the optimized duty cycle varies for the structure with different under layer thickness, the under layer thickness of 20-nm and 60-nm in Fig. 5 and Fig. 8, respectively.

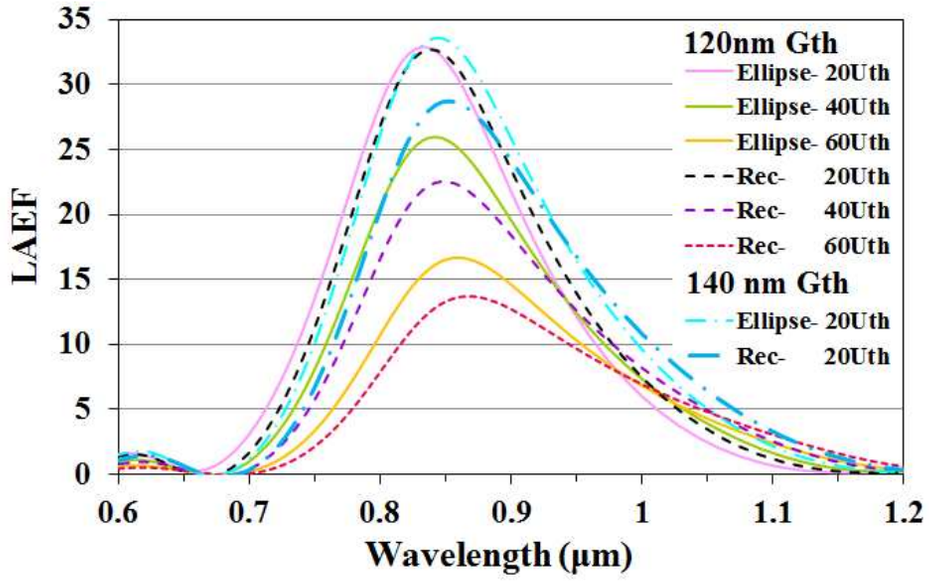

Figure 16. Light absorption enhancement factor (LAEF) calculation of different under layer thicknesses (Uth) for the rectangular and 0.9 aspect ratio ellipse-wall nano-grating structures with exponential coefficient of+5 for two different nano-grating thicknesses (Gth).

6. Conclusions

We discussed the interaction of illuminated light as electromagnetic waves through the central sub-wavelength slit on a metallic thin film surrounded by periodic nano-gratings. The concept of SPPs has been introduced and the excited SPPs are generated at metal-dielectric interface which are used for plasmonic-based applications. Plasmonics offers the ability to concentrate light into subwavelength volumes in ultra-small optoelectronic devices utilizing high-speed and broad bandwidth. Plasmonics has also made impression in nano-scale photodetector development. Photodetectors play key role in development of modern optical communication technology. Surface plasmon resonances have found practical applications in sensitive photodetectors recently. We have analyzed the performance and advantages of plasmonic-based MSM photodetectors and modeled their light absorption enhancement. The FDTD simulation tool has been used to analyze and optimize the impact of the physical and geometrical parameters on the amount of transmitted light into the MSM-PD structures. In order to maximize the flow of energy into the device active region, the performance of different nano-grating profiles and their effects on the efficiency of the photodetector have be evaluated using Drude-Lorentz dielectric function via FDTD algorithm. The corrugations on the surface lead to an effective impedance for the surface modes which favors to the resonant coupling of the SPs with incident electromagnetic wave and hence facilitates the enhancement of light transmission. The main motivation to design the nano-gratings on the MSM-PD electrodes is to assist and improve the light transmission into the slit. With the grating assisted MSM-PDs, the device could benefit the small spacing between the two top contacts, namely the central slit, for a fast response of optical pulses. The simulated results reveal that the amount of LAEF is much better than the conventional MSM-PDs. A substantial light absorption enhancement

has been found for the symmetrical MSM-PD devices. Two distinct mechanisms targeting the absorption enhancement in MSM-PDs are namely, the metal nano-gratings assisted light absorption and the subwavelength slit Fabry-Perot resonances. Feasibility of developing MSM photodetectors with high-responsivity and high-speed characteristics has made them reliable choices for high-speed optical communication systems. We have studied the transmission of TM-polarized light through subwavelength apertures in metallic films flanked by metallic nano-gratings in plasmonic-based MSM-PDs and optimized the interdigitated electrodes thicknesses and the nano-grating shapes. Simulation results confirm that the plasmonic–based grating–assisted MSM-PD is more efficient in light absorption compared with a conventional MSM-PD. The light energy confinement in the nano-scale and the produced focal point of the incident beam in plasmonic device compared with conventional MSM-PD confirm the characteristics of a nano-plasmonic lens. The demonstration of device optimization results assists to improve the concept of novel high responsivity, plasmonic-based MSM-PDs for high speed applications in optical communication. These results provide useful information for the design and fabrication of nano-scale optoelectronic devices.

Author details

Farzaneh Fadakar Masouleh[1] and Narottam Das[2,3]

1 Physics Department, University of Guilan, Rasht, Guilan, Iran

2 Department of Electrical and Computer Engineering, Curtin University, Perth, WA, Australia

3 Department of Electrical and Computer Engineering, Curtin University, Miri, Sarawak, Malaysia

References

[1] G. P. Wiederrecht. Handbook of nanoscale optics and electronics, Elsevier, Amsterdam, First edition 2010. ISBN: 978-0-12-375178-2.

[2] C. DeCusatis, and I. Kaminow. The Optical Communications Reference, Academic Press 2009. ISBN: 978-0-12-375163-8.

[3] H. Zimmermann. Silicon Optoelectronic Integrated Circuits, Springer Berlin Heidelberg 2004; 13, 1-23, doi: 10.1007/978-3-662-09904-9_1.

[4] B. P. Pal. Fundamentals of Fibre Optics in Telecommunication and Sensor Systems, bohem press, 1992.

[5] G. P. Agrawal. Fiber-Optic Communication Systems, John Wiley & Sons, Inc., Fourth Edition, 2002. doi: 10.1002/9780470918524.

[6] S. Y. Chou, Y. Liu, and P. B. Fischer. Tera-hertz GaAs metal-semiconductor-metal photodetectors with nanoscale finger spacing and width, Electron Devices Meeting, 1991. IEDM '91. Technical Digest., International, 745-748. doi: 10.1109/IEDM. 1991.235316.

[7] W. Zhang, A. K. Azad, and J. Han. Resonant Excitation of Terahertz Surface Plasmons in Subwavelength Metal Holes, Hindawi Publishing Corporation, Active and Passive Electronic Components, 2007, Article ID 40249, 8 pages, doi: 10.1155/2007/40249.

[8] R. Umeda, C. Totsuji, K. Tsuruta, and H. Totsuji. Dispersion Models and Electromagnetic FDTD Analyses of Nanostructured Metamaterials using Parallel Computer, *Memoirs of the Faculty of Engineering*, Okayama University January 2009; 43, p. 8.

[9] A. D. Rakic, A. B. Djurišic, J. M. Elazar, and M. L. Majewski. Optical Properties of Metallic Films for Vertical-Cavity Optoelectronic Devices, Applied Optics 1998; 37(22), 5271-5283. http://dx.doi.org/10.1364/AO.37.005271.

[10] M. Bordovsky et al. Waveguide design, modeling, and optimization: from photonic nanodevices to integrated photonic circuits, in Proceedings of the SPIE 5355, Integrated Optics: Devices, Materials, and Technologies VIII, 65, doi: 10.1117/12.526976, May 28, 2004.

[11] B. Ung. Study of the interaction of surface waves with a metallic nano-slit via the finite-difference time-domain method, *M.Sc. Thesis*, Laval University, Quebec, Canada, Ch. 3, 2007. http://theses.ulaval.ca/archimede/fichiers/24879/24879.html.

[12] F. F. Masouleh, N. Das, H. Mashayekhi. Impact of duty cycle and nano-grating height on the light absorption of plasmonics-based MSM photodetectors, in Proceedings of the 12th IEEE Int. Conf on Numerical Simulation of Optoelectronic Devices 2012; Shanghai, China, 13-14. doi:10.1109/NUSOD.2012.6316521.

[13] T. W. Ebbesen, H. J. Lezec, H. F. Ghaemi, T. Thio, P. A. Wolff. Extraordinary optical transmission through sub-wavelength hole arrays, Nature 1998; 391, 667-669. doi: 10.1038/35570.

[14] H. J. Lezec, A. Degiron, E. Devaux, R. A. Linke, L. Martin-Moreno, F. J. Garcia-Vidal, T. W. Ebbesen. Beaming light from a subwavelength aperture, Science 2002; 297, 820-822. doi: 10.1126/science.1071895.

[15] Y. Ding, J. Yoon, M. H. Javed, S. H. Song, R. Magnusson. Mapping surface-plasmon polaritons and cavity modes in extraordinary optical transmission, IEEE Photonics Journal 2011, 3, 365-374. doi:10.1109/JPHOT.2011.2138122.

[16] S. A. Maier. Plasmonics: Fundamentals and Applications, Springer, 2007; ISBN 978-0-387-37825-1.

[17] G. T. Reed and A. P. Knight. Silicon photonics: an introduction, John Wiley and Sons 2004; ISBN 0-470-87034-6.

[18] S. Collin, F. Pardo, R. Teissier, J. L. Pelouard. Horizontal and vertical surface resonances in transmission metallic gratings, Journal of Optics A: Pure and Applied Optics 2002; 4, 154-160. doi:10.1088/1464-4258/4/5/364.

[19] D. de Ceglia, M. A. Vincenti, M. Scalora, N. Akozbek and M. J. Bloemer. Enhancement and inhibition of transmission from metal gratings: Engineering the Spectral Response, at http://arxiv.org/abs/1006.3841, 2010.

[20] J. A. Porto, F. J. García-Vidal and J. B. Pendry. Transmission resonances on metallic gratings with very narrow slits, Physical Review Letters 1999; 83, 2845-2848. doi: http://dx.doi.org/10.1103/PhysRevLett.83.2845.

[21] A. Barbara, P. Quemerais, E. Bustarret and T. Lopez-Rios. Optical transmission through subwavelength metallic gratings, Physical Review *B* 2002; 66, Article ID 161403. doi: http://dx.doi.org/10.1103/PhysRevB.66.161403.

[22] H. Raether. Surface Plasmons on Smooth and Rough Surfaces and on Gratings, Springer-Verlag, Berlin, 1988. doi:10.1007/BFb0048323.

[23] L. Martín-Moreno, F. J. García-Vidal, H. J. Lezec, A. Degiron, and T. W. Ebbesen. Theory of highly directional emission from a single subwavelength aperture surrounded by surface corrugations, Physical Review Letters 2003; 90, Article ID 167401. doi: 10.1103/PhysRevLett.90.167401.

[24] J.A. Shackleford, R. Grote, M. Currie, J.E. Spanier, B. Nabet. Integrated plasmonic lens photodetector Appl. Phys. Lett. 2009; 94, 083501.http://dx.doi.org/10.1063/1.3086898.

[25] K. S. Yee, Numerical solution of initial boundary value problems involving maxwell's equations in isotropic media, Antennas and Propagation, IEEE Transactions on 1966; 14(3), 302-307. doi:10.1109/TAP.1966.1138693.

[26] E. Chen, and Y. S. Chou. Polarimetry of thin metal transmission gratings in the resonance region and its impact on the response of metal-semiconductor-metal photodetectors, Applied physics letters 1997; 70(20), 2673-2675. http://dx.doi.org/10.1063/1.118990.

[27] F. F. Masouleh, N. K. Das, and H. R. Mashayekhi. Assessment of amplifying effects of ridges spacing and height on nano-structured MSM photo-detectors, Journal of Optical and Quantum Electronics April 2014; 46(4). doi:10.1007/s11082-014-9900-8.

[28] N. Das, F. F. Masouleh, and H. R. Mashayekhi. A Comprehensive Analysis of Plasmonics-Based GaAs MSM-Photodetector for High Bandwidth-Product Responsivity, Advances in OptoElectronics, 2013, Article ID 793253, 10 pages, 2013. doi: 10.1155/2013/793253.

[29] N. K. Das, F. F. Masouleh, and H. R. Mashayekhi. Light Absorption and Reflection in Nano-Structured GaAs Metal-Semiconductor-Metal Photo-Detectors, IEEE Transactions on Nanotechnology Sep. 2014; 13(5), 1-8, doi: 10.1109/TNANO.2014.2336857.

[30] F. F. Masouleh, N. K. Das, and H. R. Mashayekhi. Optimization of light transmission efficiency for nano-grating assisted MSM-PDs by varying physical parameters, The Journal of Photonics and Nanostructures-Fundamentals and Applications February 2014; 12(1), 45-53. doi: 10.1016/j.photonics.2013.07.011.

[31] N. Das, A. Karar, M. Vasiliev, C.L. Tan, K. Alameh, Y.T. Lee. Analysis of nano-grating-assisted light absorption enhancement in metal–semiconductor–metal photodetectors patterned using focused ion-beam lithography, Optics Communications 2011; 284(6), 1694–1700. doi: 10.1016/j.optcom.2010.11.065.

[32] Y. Liang, W. Peng, R. Hu, and H. Zou. Extraordinary optical transmission based on subwavelength metallic grating with ellipse walls, Optics Express 2013; 21(5), 6139-6152. doi: 10.1364/OE.21.006139.

[33] F. F. Masouleh, N. K. Das, and H. R. Mashayekhi. Comparison of different plasmonic nano-grating profiles for quality light absorption in nano-structured MSM photo-detectors, Optical Engineering 2013; 52(12), 127101. doi:10.1117/1.OE.52.12.127101.